

AD-765 151

ESTIMATION OF UNMODELED FORCES ON A LUNAR
SATELLITE

B. D. Tapley, et al

Texas University

Prepared for:

Air Force Office of Scientific Research

October 1972

DISTRIBUTED BY:

NTIS

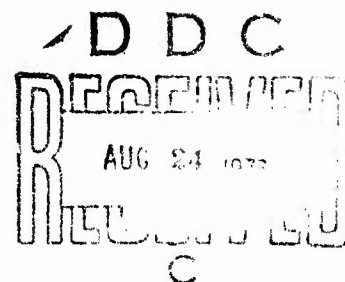
National Technical Information Service
U. S. DEPARTMENT OF COMMERCE
5285 Port Royal Road, Springfield Va. 22151

AD 765151

ESTIMATION OF UNMODELED FORCES
ON A LUNAR SATELLITE

by

B. D. Tapley and B. E. Schutz
The University of Texas at Austin



Approved for public release;
distribution unlimited.

Paper presented at the 23rd Congress of the International
Astronautical Federation, Vienna, Austria, October 8-15,
1972.

Reproduced by
NATIONAL TECHNICAL
INFORMATION SERVICE
U S Department of Commerce
Springfield VA 22151

DOCUMENT CONTROL DATA - R & D

(Security classification of title, body of abstract and indexing annotation must be entered when the overall report is classified)

1. ORIGINATING ACTIVITY (Corporate author) University of Texas at Austin Dept of Aerospace Engineerint & Engineering Mechanics Austin, Texas 78712		2a. REPORT SECURITY CLASSIFICATION UNCLASSIFIED	
3. REPORT TITLE ESTIMATION OF UNMODEIED FORCES ON A LUNAR SATELLITE		2b. GROUP	
4. DESCRIPTIVE NOTES (Type of report and inclusive dates) Scientific Interim			
5. AUTHOR(S) (First name, middle initial, last name) B. D. Tapley B. E. Schutz			
6. REPORT DATE October 1972	7a. TOTAL NO. OF PAGES 34 35	7b. NO. OF REFS 18	
6a. CONTRACT OR GRANT NO AFOSR 72-2233	8a. ORIGINATOR'S REPORT NUMBER(S)		
8. PROJECT NO 9769	9b. OTHER REPORT NO(S) (Any other numbers that may be assigned this report) AFOSR - TR - 73 - 1438.		
c. 61102F			
d. 681304			
10. DISTRIBUTION STATEMENT Approved for public release; distribution unlimited.			
11. SUPPLEMENTARY NOTES PROCEEDINGS 23rd Congress of the International Astron- autical Federation, Vienna, Austria, 8-15 Oct 72.		12. SPONSORING MILITARY ACTIVITY Air Force Office of Scientific Rsch (NM) 1400 Wilson Blvd Arlington, Virginia 22209	
13. ABSTRACT In previous investigations, a sequential estimation procedure for estimating the state of a lunar orbiting space vehicle acted upon by unmodeled terms in the lunar potential and unmodeled mechanical forces such as those due to venting has been developed. The unmodeled accelerations are approximated by a first-order Gauss-Markov process. The estimation algorithm gives an estimate of the position and velocity of the space vehicle as well as the components of the unmodeled acceleration at each observation epoch. The results obtained by processing real-time tracking data from the Apollo 10, 11, and 15 missions have indicated that the algorithm provides more precise estimates of the vehicle state than conventional orbit determination procedures and, hence, provides accurate input for navigation or guidance purposes. The question of the usefulness of the unmodeled accelerations for scientific experiments has not been established. This investigation considers the accuracy with which the algorithm can estimate the acceleration due to modeled lunar surface mascons by numerical simulation of the estimation process. It is shown that an accurate estimate of the history of the unmodeled acceleration can be obtained. The investigation also considers the effects of the magnitude and location of the mascons, as well as the effect of the observation accuracy.			

Reproduced from
best available copy.

ESTIMATION OF UNMODELED FORCES
ON A LUNAR SATELLITE[#]

by

B. D. Tapley¹ and B. E. Schutz²
Department of Aerospace Engineering
and Engineering Mechanics
The University of Texas at Austin

Abstract

In previous investigations, a sequential estimation procedure for estimating the state of a lunar orbiting space vehicle acted upon by unmodeled terms in the lunar potential and unmodeled mechanical forces such as those due to venting has been developed. The unmodeled accelerations are approximated by a first-order Gauss-Markov process. The estimation algorithm gives an estimate of the position and velocity of the space vehicle as well as the components of the unmodeled acceleration at each observation epoch. The results obtained by processing real-time tracking data from the Apollo 10, 11, and 15 missions have indicated that the algorithm provides more precise estimates of the vehicle state than conventional orbit determination procedures and, hence, provides accurate input for navigation or guidance purposes. The question of the usefulness of the unmodeled accelerations for scientific experiments has not been established.

This investigation considers the accuracy with which the algorithm can estimate the acceleration due to modeled lunar surface mascons by numerical simulation of the estimation process. It is shown that an accurate estimate of the history of the unmodeled acceleration can be obtained. The investigation also considers the effects of the magnitude and location of the mascons, as well as the effect of the observation accuracy.

¹ Professor and Chairman, Department of Aerospace Engineering and Engineering Mechanics

² Assistant Professor, Department of Aerospace Engineering and Engineering Mechanics

[#]This investigation was supported by AFOSR Grant No. 72-2233.

Introduction

The problem of estimating the state of a nonlinear dynamical system influenced by random forces using discrete observations which are subject to random error has received considerable interest during the past decade. Impetus for this interest has been derived from requirements for precise determination of the orbits and trajectories of space vehicles. The precise determination of the motion of a space vehicle is necessary, first, so that the navigation functions required to establish a specified trajectory can be performed and, second, so that measurements of the satellites' motion can be used to infer properties of the physical medium in which the vehicle is moving. The requirements of determining the motion of a lunar orbiting space vehicle have placed extensive demands on the conventional least squares orbit determination method. In particular, the problem of determining, simultaneously, precise estimates of the vehicle position and velocity while estimating the values for the coefficients of the lunar gravity field may require accuracies which exceed the capabilities of classical orbit determination methods.

The solution to the classical orbit determination problem involves linearizing the nonlinear equations, which define the problem, about a specified reference trajectory and then applying linear estimation techniques. Once the problem has been reduced to a linear estimation problem, the estimation algorithm is obtained by applying the weighted least squares method or by use of statistical based estimation methods, such as minimum variance or maximum likelihood methods. Using the results from either of these approaches, the estimate may be obtained by using a batch data processing algorithm, in which all of the observations are processed simultaneously to obtain an estimate of the state at some reference epoch, or the state estimate may be obtained by processing each data point sequentially as it is obtained.

It is well known that errors of four basic types influence the accuracy of the estimate obtained by each of these procedures; i.e., 1) errors due to the linearization assumptions, 2) errors introduced in the computational procedure, 3) errors which occur in the observation process, and 4) errors due to inaccuracies in the mathematical model used to define the problem. The effect of these errors on batch-type estimation algorithms is discussed in Ref. (1), (2), and (3). If the extended form of the sequential estimation algorithm⁽⁴⁾ is used, where the estimate of the state at a time, t_i , is used to define the reference trajectory for propagating the estimate from the observation epoch, t_i , to the next observation epoch, t_j , the effects of the nonlinearities are minimized. Furthermore, in most orbit determination problems, sufficient accuracy can be obtained during the computation process to eliminate the integration errors. Hence, using the extended sequential estimation algorithm, the effects of the last two error sources will be the primary factors which limit the orbit determination accuracy for near-earth or near-lunar satellites. While the effects of the observation errors are an important factor, the increase in the accuracy of the doppler tracking data coupled with the high precision laser ranging data suggests that errors in the data are less important in limiting the accuracy obtained with conventional orbit determination procedures than are the errors due to model inaccuracies. As a consequence of this fact, primary attention in this investigation will be directed towards consideration of methods for reducing the errors due to inaccuracies in the dynamic model.

It should be noted that there is some trade-off between the errors which occur in the computational process and the errors due to an incomplete or inaccurate mathematical model. With a more complete mathematical model, it is more difficult to obtain an accurate numerical solution to the relations which define the estimation procedure. On the other hand, if the mathematical model is simplified to

alleviate the computational problems, important physical effects may be neglected. The subsequent estimation procedure may "diverge" due to model error⁽¹⁾⁽⁵⁾. This difficulty may be encountered, also, if the actual dynamical process is not understood well enough to allow a precise definition of the mathematical model. The effects of inaccuracies in the mathematical model on the accuracy and the stability of the linear sequential estimation procedures are discussed in Ref. (4), (5), and (6). A number of methods have been proposed to alleviate the problem of estimation divergence. These methods include additions to the state error covariance matrix to account for noise in the differential equations which govern the motion⁽⁷⁾, specification of a minimum bound on the estimation error covariance matrix⁽⁸⁾, and the utilization of a finite⁽⁴⁾ or decaying⁽⁹⁾ data set. While these methods lead to a more stable estimation algorithm, they suffer from the disadvantage that the accuracy of the estimate is determined by certain empirical parameters which must be specified "a priori" without knowledge of the disturbing process. In addition, the methods do not yield information directly related to the unmodeled accelerations. Such information is of considerable value in post-flight data analysis for improving the knowledge of the mathematical model.

In the following discussion, a sequential estimation method which compensates for unmodeled effects in the differential equations of the dynamical process, is described. The method has two advantages: 1) it can be used to obtain an improved estimate of the vehicle state during real time estimation problems and 2) the method will yield information which can be used in post-flight data analysis to improve the mathematical model. In the proposed method, the "unmodeled" accelerations are assumed to consist of the superposition of a time correlated component and a purely random component and are approximated by a first-order Gauss-Markov process. This model has been used previously to compensate for

errors in inertial navigation devices⁽¹⁰⁾, and to compensate for the effects of random fluctuations in atmospheric drag⁽¹¹⁾.

In Refs. (10) and (11), a stationary Gauss-Markov process is assumed and the correlation time, or equivalently, the correlation coefficient is assumed to be constant and known, apriori. In Refs. (12) and (13), this assumption is relaxed and the correlation coefficients are regarded as unknown parameters and the best estimate of their values are determined during the estimation process. In Refs. (12) and (13), this approach is used to develop a sequential estimation procedure for estimating the state of a lunar orbiting space vehicle acted upon by unmodeled forces due to an incomplete lunar potential and unmodeled mechanical forces such as those due to venting, water dumps, or translational forces due to unbalanced attitude control reactions. The estimation algorithm gives an estimate of the position and velocity of the space vehicle as well as the components of the unmodeled acceleration at each observation epoch. The algorithm, referred to as the Dynamic Model Compensation (DMC) method, has been applied in further simulated studies in Refs. (14) and (15). The results of these studies along with the results from processing real time tracking data from the Apollo 10, 11, and 15 missions⁽¹²⁾⁽¹³⁾ have indicated that the algorithm provides more precise estimates of the vehicle state than the conventional least squares batch or sequential orbit determination procedures and, hence, provides a more accurate input for navigation or guidance purposes. The results obtained in these studies indicate that the estimation procedure is stable in the sense that the error norm does not grow in an unbounded manner and that the norm of the covariance matrix provides a conservative bound on the error in the estimate. Finally, the estimates of the unmodeled accelerations obtained by processing range-rate tracking data from the lunar orbit phase of the Apollo 10 and 11 missions indicated a high

correlation with the location of lunar surface mass concentrations, as reported in Refs. (12) and (13). In these studies the observation residual was bounded by the formal standard deviation assigned to the range-rate measurements and, consequently, it is conjectured that the estimates of the unmodeled accelerations are reasonable representations of the true unmodeled accelerations acting on the vehicle. However, since actual tracking data is used for the studies reported in Refs. (12) and (13), the true acceleration history is not available for comparison.

The primary objective of the investigation described in the following sections is to determine the accuracy with which the unmodeled accelerations can be estimated using the Dynamic Model Compensation (DMC) method proposed in Refs. (12) and (13). The question is answered by simulating numerically the orbit determination procedure for a space vehicle in an Apollo-type lunar orbit. In the simulated study, consideration is given to the effects of the accuracy and density of the observations, as well as the magnitude of the unmodeled accelerations, on the accuracy of the estimate.

The Estimation Algorithm

The equations which describe the motion of a lunar satellite can be expressed by the following system of first-order differential equations:

$$\dot{\mathbf{r}} = \mathbf{v}, \quad \dot{\mathbf{v}} = \mathbf{a}_c + \mathbf{a}_p + \mathbf{m} \quad (1)$$

where \mathbf{r} is a three-vector of selenocentric position components, \mathbf{v} is a three-vector of selenocentric velocity components, \mathbf{a}_c is the acceleration due to the central body, \mathbf{a}_p is the modeled acceleration due to other sources, gravitational or otherwise, and, the three-vector, \mathbf{m} , represents the effects of all accelerations not accounted for in the mathematical model used to describe the motion of the satellite. In the subsequent consideration, \mathbf{m} will be referred to as the "unmodeled acceleration".

In the Dynamic Model Compensation procedure described in the following discussion, the unmodeled acceleration \mathbf{m} is approximated as an adaptive, first-order, Gauss-Markov process, $\epsilon(t)$, which satisfies the following vector differential equation

$$\dot{\epsilon}(t) = \mathbf{B}\epsilon(t) + \mathbf{u}(t) \quad (2)$$

where $\epsilon(t)$ is a three-vector whose components approximate the values of the unmodeled accelerations at the time, t , and $\mathbf{u}(t)$ is a three-vector of Gaussian noise whose components are assumed to satisfy the apriori statistics:

$$E[\mathbf{u}(t)] = \mathbf{0}, \quad E[\mathbf{u}(t)\mathbf{u}^T(\tau)] = \mathbf{q}(t)\delta(t - \tau) \quad (3)$$

where $\delta(t - \tau)$ is the Dirac "Delta" function and where $\mathbf{q}(t)$ is assumed to be a diagonal matrix. This assumption implies that the components of \mathbf{u} are not correlated. The coefficient matrix, \mathbf{B} , is defined by the components $B_{ij} = \beta_i \delta_{ij}$ ($i, j = 1, 2, 3$) where the β_i are assumed to be unknown parameters whose

values are to be determined during the estimation process by the inclusion of the equation $\dot{\beta} = 0$, where $\beta^T = [\beta_1 \beta_2 \beta_3]$. If ϵ is substituted for m in Eq. (1) and if the state vector X is defined as

$$X^T = [r^T : v^T : \epsilon^T : \beta^T] \quad (4)$$

then Eqs. (1), (2), and the relations $\dot{\beta} = 0$ can be combined to obtain the following differential equations for the state of the dynamical system:

$$\dot{X} = F(X, u, t), \quad X(t_0) = X_0 \quad (5)$$

where $F^T = [v^T : (a_m + \epsilon)^T : (B\epsilon + u)^T : 0]$ and where $a_m = a_c + a_p$, i.e., the components of the modeled acceleration. In the usual orbit determination problem, the initial conditions, X_0 , are unknown.

For $t > t_i$, where t_i is some reference epoch, the solution to Eq. (5) can be expressed in integral form as follows:

$$\begin{aligned} r(t) &= r_i + v_i \Delta t + \int_{t_i}^t a(\tau) [t - \tau] d\tau \\ v(t) &= v_i \Delta t + \int_{t_i}^t a(\tau) d\tau \\ \epsilon(t) &= E(t) \epsilon_i + l_1, \quad \beta(t) = \beta_i \end{aligned} \quad (6)$$

where $\Delta t = t - t_i$ and $a(t) = a_m(t) + \epsilon(t)$. The matrices $E(t)$ and l_1 are defined as

$$E(t) = \begin{bmatrix} \alpha_x & 0 & 0 \\ 0 & \alpha_y & 0 \\ 0 & 0 & \alpha_x \end{bmatrix} \quad (7)$$

$$\mathbf{l}_i^T = [\sigma_x \sqrt{1-\alpha_x^2} u_x : \sigma_y \sqrt{1-\alpha_y^2} u_y : \sigma_z \sqrt{1-\alpha_z^2} u_z] \quad (8)$$

where $\alpha_x = \exp[-\beta_x(t - t_i)]$ with similar definitions for α_y and α_z .

Further details on the development of the third of Eqs. (6) are given in Ref. (16).

Using the definition in Eq. (4), the solution to Eqs. (5) can be expressed as

$$\mathbf{X}(t) = \theta(\mathbf{X}_i, t_i, t) + \boldsymbol{\eta}_i, \quad t \geq t_i \quad (9)$$

where $\boldsymbol{\eta}_i^T = [\eta_r^T : \eta_v^T : \eta_e^T : 0]$. The components of the state noise matrix, $\boldsymbol{\eta}_i$, are due to the purely random components of the unmodeled accelerations and can be defined as follows:

$$\eta_r = \int_{t_i}^t \ell_i(t - \tau) d\tau, \quad \eta_v = \int_{t_i}^t \ell_i d\tau, \quad \eta_e = \ell_i \quad (10)$$

In view of Eqs. (3), the random process $\boldsymbol{\eta}_i$ will satisfy the conditions

$$E[\boldsymbol{\eta}_i] = 0, \quad E[\boldsymbol{\eta}_i \boldsymbol{\eta}_j^T] = \mathbf{Q}_i \delta_{ij} \quad (11)$$

where δ_{ij} is the Kronecker delta. Eq. (9) is used to propagate the state vector from an observation point t_i to an observation point t_j .

The relationship between the p -dimensional observation vector \mathbf{Y}_i , the p -vector of observation noise, \mathbf{v}_i , and the state at the time, t_i , is

$$\mathbf{Y}_i = \mathbf{G}(\mathbf{X}_i, t_i) + \mathbf{v}_i \quad (12)$$

In the following discussion, it is assumed that the observation noise, \mathbf{v}_i , satisfies the following conditions:

$$E[\mathbf{v}_i] = 0, \quad E[\mathbf{v}_i \mathbf{v}_j^T] = \mathbf{R}_i \delta_{ij}, \quad E[\mathbf{v}_i \mathbf{X}_j^T] = 0 \quad (13)$$

where δ_{ij} is the Kronecker delta.

The problem considered then is posed as follows: Given the relation for propagating the state, Eq. (9), the observation-state relation, Eq. (12), the sequence of observations Y_i , $i = 1, \dots, k$, and the statistics on the state noise, Eq. (3), and the observation noise, Eq. (13), find the best estimate, in the minimum variance sense, of the state, \hat{X}_k , at the time t_k .

Under the conditions given in the previous problem, the estimate at the time, t_k , can be obtained using the following algorithm⁽⁴⁾:

$$\begin{aligned}\bar{X}_k &= \theta(\hat{X}_{k-1}, t_{k-1}, t_k) \\ \bar{P}_k &= \phi(t_k, t_{k-1}) P_{k-1} \phi^T(t_k, t_{k-1}) + Q_{k-1} \\ K_k &= \bar{P}_k H_k^T [H_k \bar{P}_k H_k^T + R_k]^{-1} \\ \hat{X}_k &= \bar{X}_k + K_k [Y_k - G(\bar{X}_k, t_k)] \\ P_k &= [I - K_k H_k] \bar{P}_k\end{aligned}\tag{14}$$

where $H_k = [\partial G / \partial X]^*$, $\bar{X}_k = E[X_k | Y_1, \dots, Y_{k-1}]$ and $\hat{X}_k = E[X_k | Y_1, \dots, Y_k]$. The covariance matrices \bar{P}_k and P_k are associated with the state estimates \bar{X}_k and \hat{X}_k , respectively. The state transition matrix, $\phi(t_k, t_{k-1})$ satisfies the following differential equation

$$\dot{\phi}(t, t_k) = A(t) \phi(t, t_k); \quad \phi(t_k, t_k) = I\tag{15}$$

where $A(t) = [\partial F / \partial X]^*$. The symbol $[]^*$ indicates that the quantity in the bracket is evaluated on the solution, $\bar{X}(t) = \theta(\hat{X}_{k-1}, t_{k-1}, t)$, $t_k \leq t$. The solution $\theta(\hat{X}_{k-1}, t_{k-1}, t)$ is obtained from Eq. (9) using the condition that $\bar{X} = E[\bar{X} | Y_1, \dots, Y_{k-1}] = 0$. The algorithm given by Eqs. (14) and (15) is the extended form of the usual linear sequential estimator or the Kalman-Bucy filter

as discussed in Ref. (4). The covariance matrix P_k is associated with the best estimate of X_k based on k -observations while \bar{P}_k is the covariance matrix associated with the best estimate of X_k based on $(k-1)$ -observations.

It should be recalled that the estimate \hat{X}_k , includes an estimate at the time, t_k , of the components of the position, the velocity, the unmodeled acceleration, ϵ , and the correlation coefficients, β_x , β_y , and β_z . The algorithm requires apriori or "initial" estimates of each of these quantities as well as the apriori covariance matrices, P_0 , Q_1 , and R_1 , associated with the initial state error and with the state noise and the observation noise, respectively. The development of the algorithm and the computational procedure required to implement the algorithm are discussed in greater detail in Refs. (12) and (13).

In addition to processing the tracking data from the Apollo 10 and 11 missions, the investigation described in Refs. (12) and (13) evaluate the characteristics of the estimation algorithm using simulated data. It is concluded from the simulated studies that in the presence of the unmodeled accelerations, the algorithm is stable and the covariance matrix provides a reasonable, but conservative estimate of the actual error. Furthermore, the estimate of the position and velocity is more accurate than the estimate obtained using the usual sequential estimator or Kalman Filter, modified as discussed in Ref. (4), to account for the effects of state process noise. In the simulated study which follows, the accuracy with which the unmodeled acceleration components can be estimated by the DMC procedure is investigated.

Generation of the Simulated Observations

The simulated observations are generated by the integration of the system of equations

$$\dot{r}_T = v_T, \quad \dot{v}_T = a_m + m \quad (16)$$

where $r_T(t_0)$, $v_T(t_0)$ and $m(t)$ are specified and where in the simulated study r_T represents a three-vector of the true position components, v_T is a three-vector of the true velocity components, a_m represents the terms modeled in the estimation algorithm, and m represents the terms not directly included in the dynamic model used in the estimation algorithm. The term m will define the true model error and is approximated by a first-order Gauss-Markov process in the DMC estimation algorithm. The model error is simulated in the following study by assuming that m is the acceleration due to several point masses at various locations on the lunar surface. In the simulation, the term a_m includes the central body acceleration of the moon and the acceleration due to a point-mass earth. The effects of the sun and the other planets were neglected.

The numerical integration of Eq. (16) yields a solution for the "true" motion of the satellite which is used in generating simulated observations. The computer program ascertains which tracking stations can observe the satellite and a range-rate observation, $\dot{\rho}$, is generated using the position and velocity of the satellite relative to a topocentric earth-fixed tracking station. The "true" value of the range-rate observation is corrupted to simulate the actual observation by adding the quantity $\sigma_{\dot{\rho}} \lambda$, where $\sigma_{\dot{\rho}}$ is the standard deviation of the observation noise and λ is a Gaussian distributed random variable with zero mean and unit variance.

The numerical integration used in both the simulations and the estimation procedure is a variable step Runge-Kutta method formulated in Ref. (18). As implemented, integrators of two different orders can be used. During periods in which observations are generated, a fixed step size is used to simulate a fixed observation interval. This interval is normally sufficiently small to allow use of a lower order integrator, namely, the Runge-Kutta-Fehlberg 4(5). If the observation interval results in a step size which is too large and the 4(5) is inadequate for maintaining accuracy, a higher order 7(8) method can be used.

The estimation program requires the numerical integration of Eqs. (5) and (15), whereas the observation generation requires the integration of Eq. (16), only. The state vector for Eq. (5) consists of 12 elements, while Eq. (16) involves six elements. The state transition matrix, defined in Eq. (15), consists of 144 elements; however, the order of the system can be reduced by noting that a number of elements can be integrated analytically.

To simulate the real-world, the nominal or reference orbit initial conditions were assumed to be different from those used in the generation of the observations. The differences between the two sets of initial conditions for all orbits considered, were as follows:

$$\begin{array}{ll} \Delta x = -305.8 \text{ meters} , & \Delta \dot{x} = 0.0542 \text{ meters/sec} \\ \Delta y = -304.7 \text{ meters} , & \Delta \dot{y} = -0.3682 \text{ meters/sec} \\ \Delta z = -71.9 \text{ meters} , & \Delta \dot{z} = 0.3135 \text{ meters/sec} \end{array}$$

Two orbit inclinations were considered, i.e., $I = 180^\circ$ and $I = 150^\circ$. For both cases, the satellite starts at approximately 90° East selenographic longitude, with altitude of 100 km, and with an eccentricity of zero. For the case $I = 180^\circ$, the satellite will be in a lunar equatorial orbit. The lunar groundtrack of the

inclined orbit is shown in Fig. 1. Fig. 1 also shows the locations of four mascons whose effect was included in the generation of the simulated observations, but was not included in the dynamic model, a_m , for the estimation algorithm. The figure on which the simulated groundtrack is drawn (Fig. 1) was provided by W. L. Sjogren of the Jet Propulsion Laboratory¹⁸.

The simulated mascons shown in Fig. 1 are given in Ref. (18). (See also Table I). It should be noted that the gravity contours in Ref. (18) are line-of-sight accelerations between the satellite and the ground station. These line-of-sight accelerations are normalized to 100 km above the mean lunar surface.

Table I

<u>Mascon Name</u>	<u>Lat. (Deg.)</u>	<u>Long. (Deg.)</u>	<u>Mass ($\times 10^{-6}$ Lunar Mass)</u>
1. Imbrium	+38	-18	20
2. Serenitatis	+28	+18	20
3. Crisium	+16	+58	10
4. Nectaris	-16	+34	9

The DMC method estimates the unmodeled acceleration vector which is plotted in the local spacecraft coordinate system shown in Fig. 2. In this figure, λ is the selenographic longitude and ϕ is the latitude. The unit vector \bar{e}_r lies along the selenocentric position vector of the satellite, unit vector \bar{e}_ϕ is directed due east, and \bar{e}_λ is along the spacecraft latitude meridian. The locations of the tracking stations coincide with those used in the Apollo missions. Generally, between four and seven stations can observe the satellite simultaneously.

In all cases, the initial covariance matrix, P_0 , was assumed to be diagonal with the following initial values: $P_{xx} = P_{yy} = P_{zz} = \sigma_r^2 = 9 \times 10^4$ (meters)², $P_{\dot{x}\dot{x}} = P_{\dot{y}\dot{y}} = P_{\dot{z}\dot{z}} = (\sigma_v)^2 = .25$ (meters/sec)², $P_{\epsilon_x \epsilon_x} = P_{\epsilon_y \epsilon_y} = P_{\epsilon_z \epsilon_z} = 4 \times 10^{-8}$ (meters/sec²)² and $P_{\beta_x \beta_x} = P_{\beta_y \beta_y} = P_{\beta_z \beta_z} = 2.25 \times 10^{-4}$ sec². The initial value of \bar{e} is assumed to be zero. Finally, an observation interval of six seconds was used.

Numerical Results

The results obtained in the simulated study compare the behavior of the extended Kalman-Bucy filter with no model compensation with the behavior of the DMC method for both an equatorial orbit and an inclined orbit. The effect of the observation accuracy and the unmodeled acceleration magnitude are considered. As described in the previous section, the true model error is due to the four lunar surface mascons.

1. Behavior With No Model Compensation

For this case, the observations were generated by including the mascons; however, in the estimation algorithm, they were neglected in the model used for a_m . The effects of the unmodeled accelerations were not accounted for through the use of the state noise covariance matrix Q in Eq. (15). This case then represents the application of the extended form of the Kalman-Bucy filter with no model compensation. The observation accuracy is 1.5 mm/sec. For the retrograde equatorial orbit ($I = 180^\circ$), the position and velocity error norms are shown in Fig. 3. Since this is a simulation, the actual error in the estimate is known from

$$\Delta r = \sqrt{(\hat{x} - x_T)^2 + (\hat{y} - y_T)^2 + (\hat{z} - z_T)^2}$$

where the $(\hat{})$ indicates estimated values, and $()_T$ indicates true values used in generating the observations. Fig. 3 also shows a plot of the square root of the trace of the first three diagonal elements of the covariance matrix P , i.e.,

$$P_r = \sqrt{P_{xx} + P_{yy} + P_{zz}}$$

Note that the actual error is not bounded by the covariance matrix. With no model compensation, the actual position error norm reaches a maximum of over 600 meters and the velocity error norm has a peak at .5 meters/sec. The orbit with

$I = 150^\circ$ passes directly over two of the simulated mascons. With no model compensation, the error norms are shown in Fig. 4. The position error reaches a value of 10,000 meters. The estimation procedure has diverged for this case.

The position and velocity error norms are shown in lieu of observation residuals. The residuals show the effect of a systematic error and will have a pseudo-periodic behavior. Due to the number of stations involved, the residuals would require several plots whereas the error norm requires only two plots. Finally, it should be noted that application of the batch processor to these two orbits will yield residuals of comparable magnitude and pseudo-periodic character. See, for example, the results given in Ref. (14).

2. Behavior Using the DMC Method

Application of the DMC method to the $I = 180^\circ$ case yields the results shown in Fig. 5. Figure 5a shows the radial-component of the unmodeled acceleration compared with the estimate provided by the DMC algorithm. The smooth line is the true acceleration and the uneven line is the estimate of the true acceleration. Figures 5b and 5c show the $\bar{\xi}_\lambda$ and $\bar{\xi}_\phi$ components. The acceleration unit used in these plots is the milligal (mgal). Note that the DMC method provides a very good estimate of the unmodeled acceleration. The position error norm is illustrated in Fig. 5d and the velocity error norm in Fig. 5e. It can be seen from Fig. 5d that the smooth line, the square root of the trace of the first three elements in the covariance matrix, P , represents a conservative estimate of the position error and that the estimate of the state of the satellite is improved considerably over the estimate obtained in the preceding case, i.e., with no model compensation. The observation noise standard deviation used in both the simulation and estimation computations was 1.5 mm/sec as in the preceding case.

For the $I = 150^\circ$ case, the acceleration estimates are shown in Fig. 6a to 6c. Since the satellite passes almost directly over the location of two of the simulated mascons, the unmodeled acceleration is almost 100 times larger than for the equatorial orbit. The acceleration estimates again yield accurate approximations of the true acceleration. Furthermore, it can be seen from Fig. 6d that the covariance matrix provides a conservative estimate of the actual error. In Fig. 6e, the true velocity error norm is scattered about the covariance matrix, thus the covariance is indicative of the actual velocity error. The observation standard deviation for this case was 1.5 mm/sec.

3. Effect of Improved Observation Accuracy on the DMC Method

To evaluate the influence of observation accuracy, the case, $I = 150^\circ$, was recomputed with an observation error standard deviation of 0.15 mm/sec, i.e., an improvement over the previous case of an order of magnitude. The results are given in Fig. 7. In Figs. 7a through 7c, a dramatic improvement in the accuracy of the estimate of the unmodeled acceleration can be seen. Furthermore, as one would expect, an improvement in the estimate of the position and velocity of the satellite also occurs. Similar behavior occurs for the $I = 180^\circ$ orbit.

Summary and Conclusions

The results of the preceding section demonstrate that the DMC algorithm can provide more accurate estimates of the state than can be obtained with the non-compensated algorithms. Furthermore, the method provides estimates of the unmodeled acceleration time-history which are representative of the true unmodeled acceleration. The accuracy of the acceleration estimate depends on the magnitude of the unmodeled acceleration, the accuracy of the observations and density of the observation data set, i.e., the number of tracking stations observing the satellite.

For a sufficiently large value of the ratio of the magnitude of the unmodeled accelerations to the accuracy of the observations and for a sufficiently dense observation data set, a precise estimate of the components of the unmodeled accelerations can be obtained by the Dynamic Model Compensation algorithm described in this investigation. The estimates of the components of the unmodeled accelerations can be used to improve the knowledge of the lunar gravitational potential representation.

References

1. Squires, R. K., et al, "Response of Orbit Determination Systems to Model Errors," C-643-69-503, Goddard Space Flight Center, Greenbelt, Md., 1969.
2. Gapcynski, J. P., W. T. Blackshear, and H. R. Campton, "The Lunar Gravitational Field as Determined from the Tracking Data of the Lunar Orbiter Series of Spacecraft," AAS/AIAA Astrodynamics Specialist Conference, AAS Paper No. 68-132, Jackson, Wyoming, Sept., 1968.
3. Hamer, H. A. and K. G. Johnson, "Effect of Gravitational-Model Selection on the Accuracy of Lunar Orbit Determination from Short Data Arcs," NASA TN D-5105, Langley Research Center, March, 1969.
4. Jazwinski, A. H., Stochastic Processes and Filtering Theory, Academic Press, New York, New York, 1969, pp. 276-277.
5. Schlee, F. H., C. J. Standish, and N. F. Toda, "Divergence in the Kalman Filtering," AIAA Journal, Vol. 5, No. 6, June, 1967, pp. 1114-1120.
6. Schmidt, S. F., "Computational Techniques in Kalman Filtering Theory," Theory and Applications of Kalman Filtering, NATO AGARDograph 139, Ed. by C. T. Leondes, February, 1970, Chapter 3.
7. Sorenson, H. W., "Kalman Filtering Techniques," Advances in Control Systems, Vol. 3, Ed. by C. T. Leondes, 1966, pp. 219-292.
8. Potter, J. E. and J. C. Decker, "The Minimal Bound on the Estimation Error Covariance Matrix in the Presence of Correlated Driving Noise," SIAM Jr. Control, Vol. 8, pp. 513-526, Nov., 1970.
9. Miller, R. W., "Asymptotic Behavior of the Kalman Filter with Exponential Aging," AIAA Jr., Vol. 9, pp. 537-539, March, 1971.
10. Fitzgerald, R. J., "Filtering Horizon-Sensor Measurements for Orbital Navigation," Proc. of AIAA/JACC Guidance and Control Conference, Seattle, Washington, Aug., 1966, pp. 500-599.
11. Rauch, H. E., "Optimum Estimation of Satellite Trajectories Including Random Fluctuations in Drag," AIAA Jr., Vol. 3, No. 4, April, 1965, pp. 717-722.
12. Ingram, D. S., and B. D. Tapley, "Estimation of Unmodeled Forces on a Lunar Satellite," AAS/AIAA Astrodynamics Specialist Conference, Paper No. 71-371, 1971.
13. Tapley, B. D. and D. S. Ingram, "Orbit Determination in the Presence of Unmodeled Accelerations," Proc. of the Second Symposium on Nonlinear Estimation Theory, San Diego, Calif., Sept., 1971.
14. Schutz, B. E., B. D. Tapley, and P. E. Connolly, "Orbit Determination of Satellites in the Presence of Geopotential Model Errors," Proc. of the International Symposium on Earth Gravity Models and Related Problems, St. Louis, Missouri, Aug., 1972.

15. Tapley, B. D., and H. Hagar, Jr., "Estimation of Unmodeled Forces on a Low-Thrust Space Vehicle," Proc. of the Third Symposium on Nonlinear Estimation Theory, San Diego, California, Sept., 1972.
16. Doob, J. L., "The Brownian Movement and Stochastic Equations," Annals. of Mathematics, Vol. 43, No. 2, April, 1942, pp. 351-369.
17. Muller, P. M. and W. L. Sjogren, "Lunar Gravimetry and Mascons," Applied Mechanics Reviews 22, No. 9, September, 1969.
18. Fehlberg, E., "Classical Fifth-, Sixth-, Seventh-, and Eighth-Order Runge-Kutta Formulas with Stepsize Control," NASA TR R-287, 1968.

CONTOUR INTERVAL = 10 m/sec
 MAP PROJECTION = SPHERICAL PROJECTION
 L. D. S. ACCELERATION NORMALIZED
 AT 100 L. ABOVE SURFACE

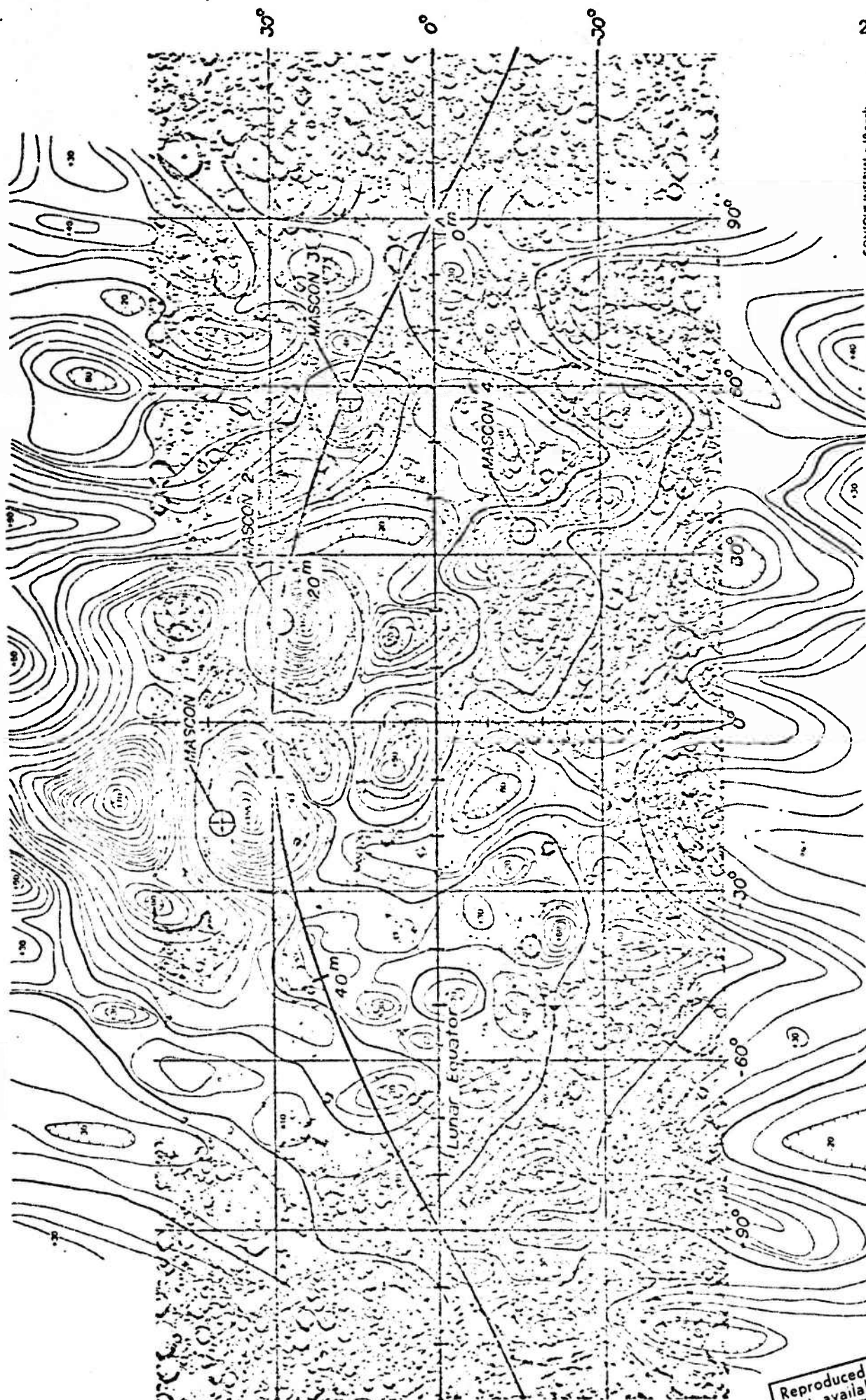


FIGURE 1. SIMULATED LUNAR SATELLITE GROUND TRACK

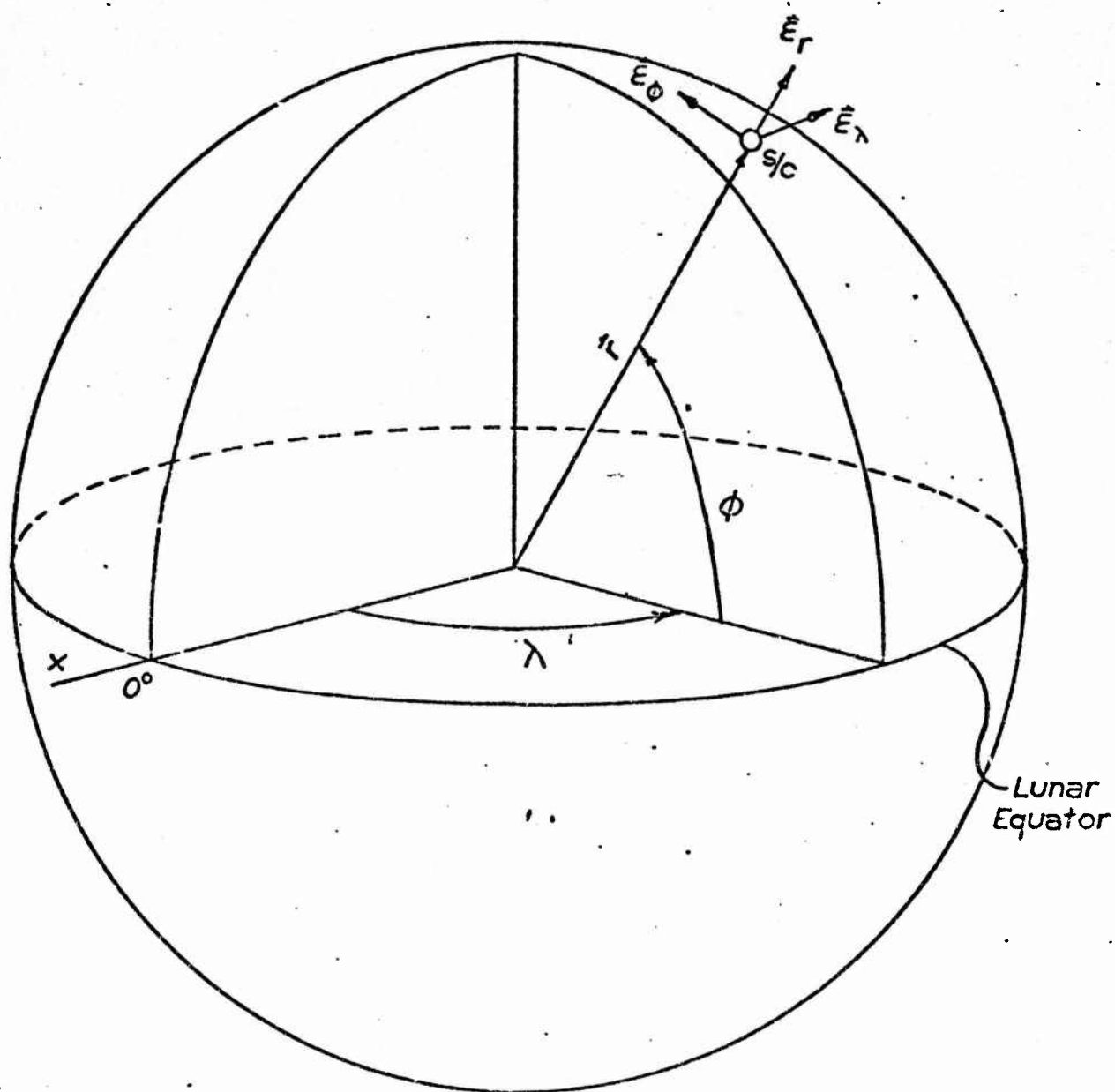
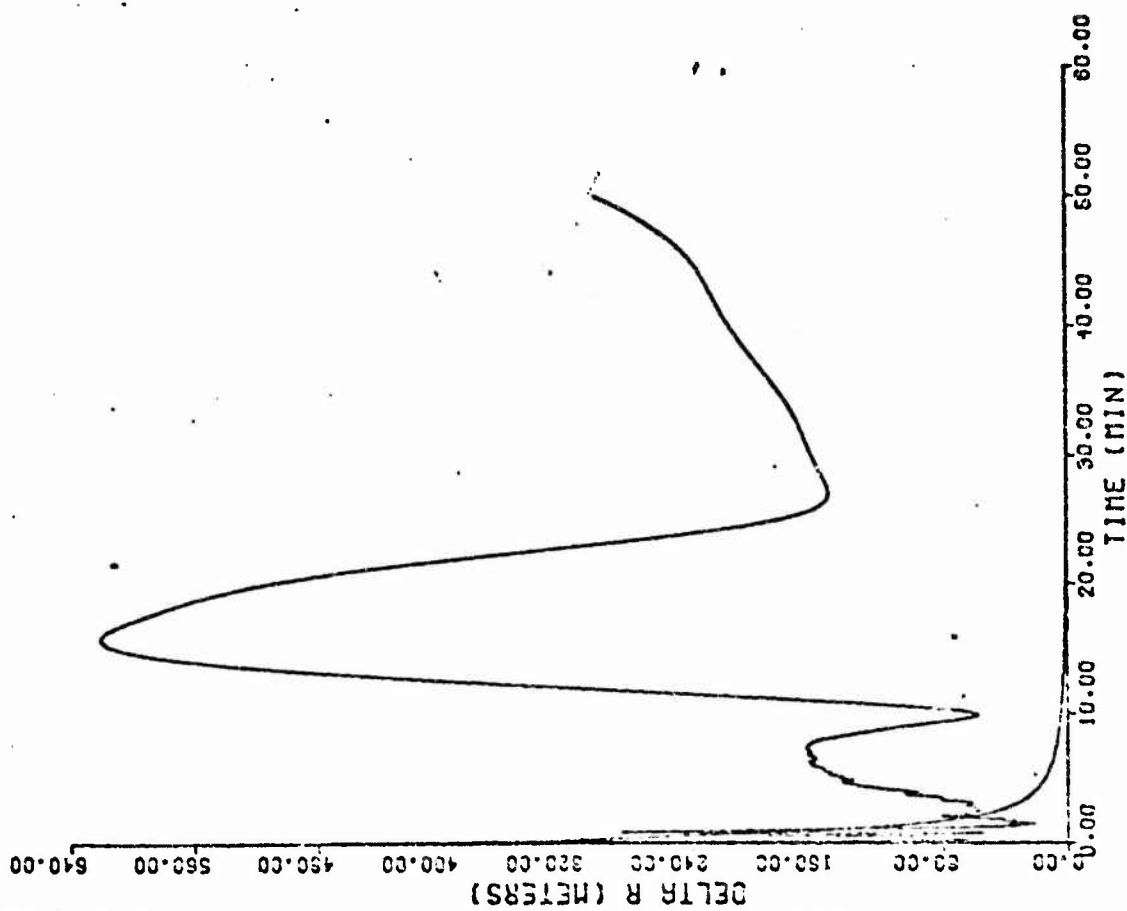
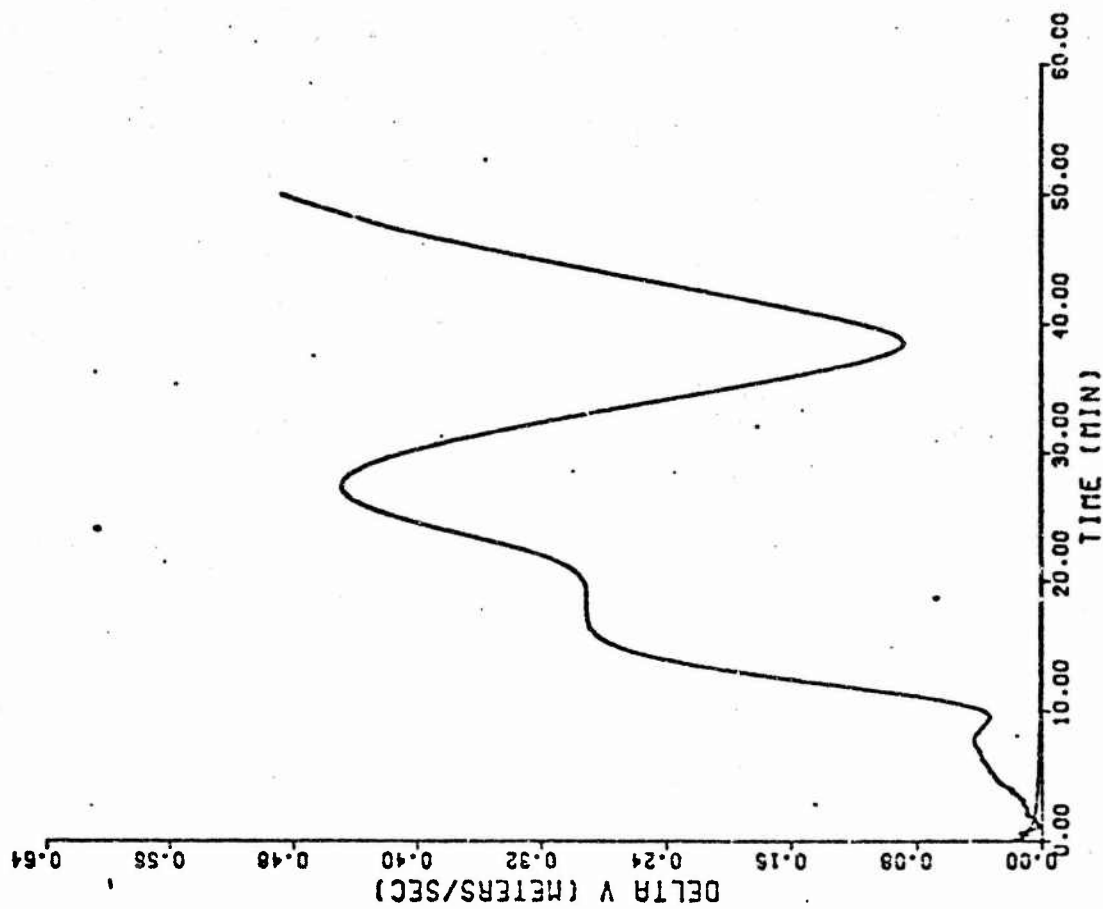


FIGURE 2. UNMODELED ACCELERATION COORDINATE SYSTEM

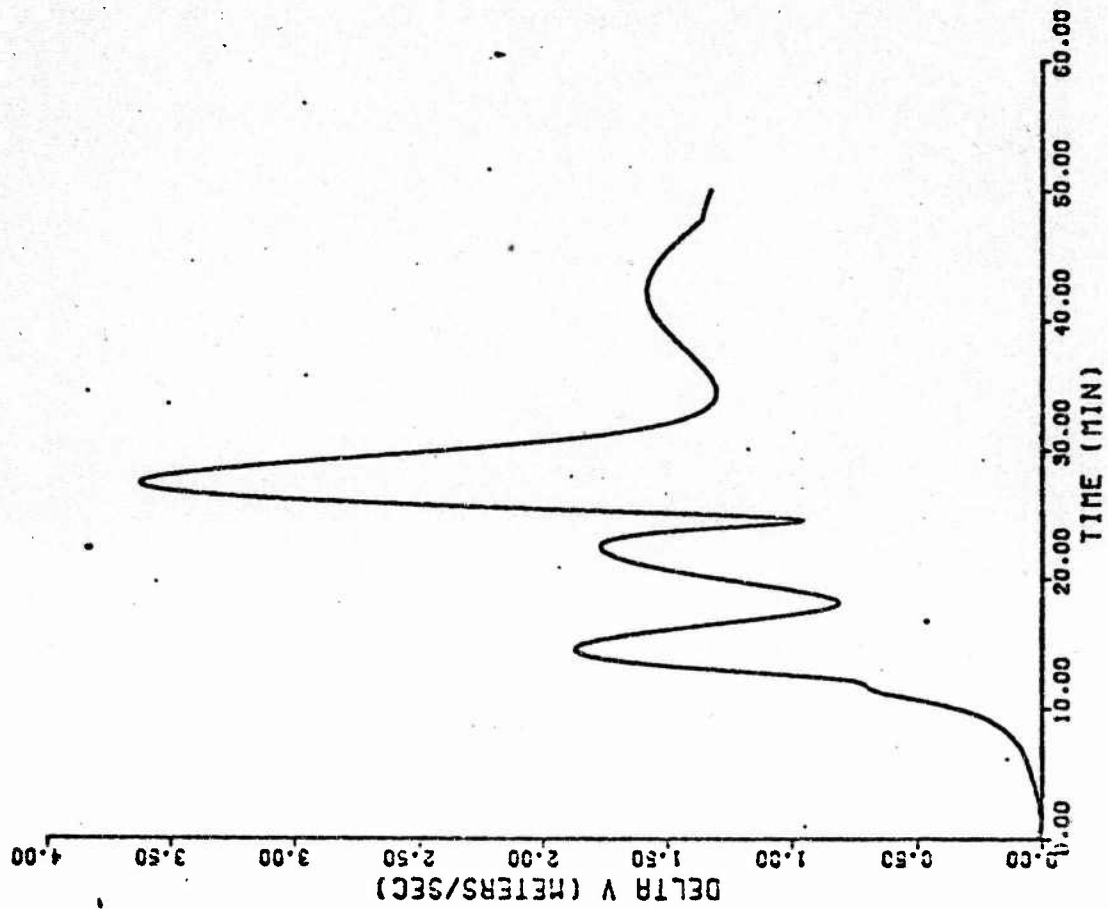


a. Position Error Norm

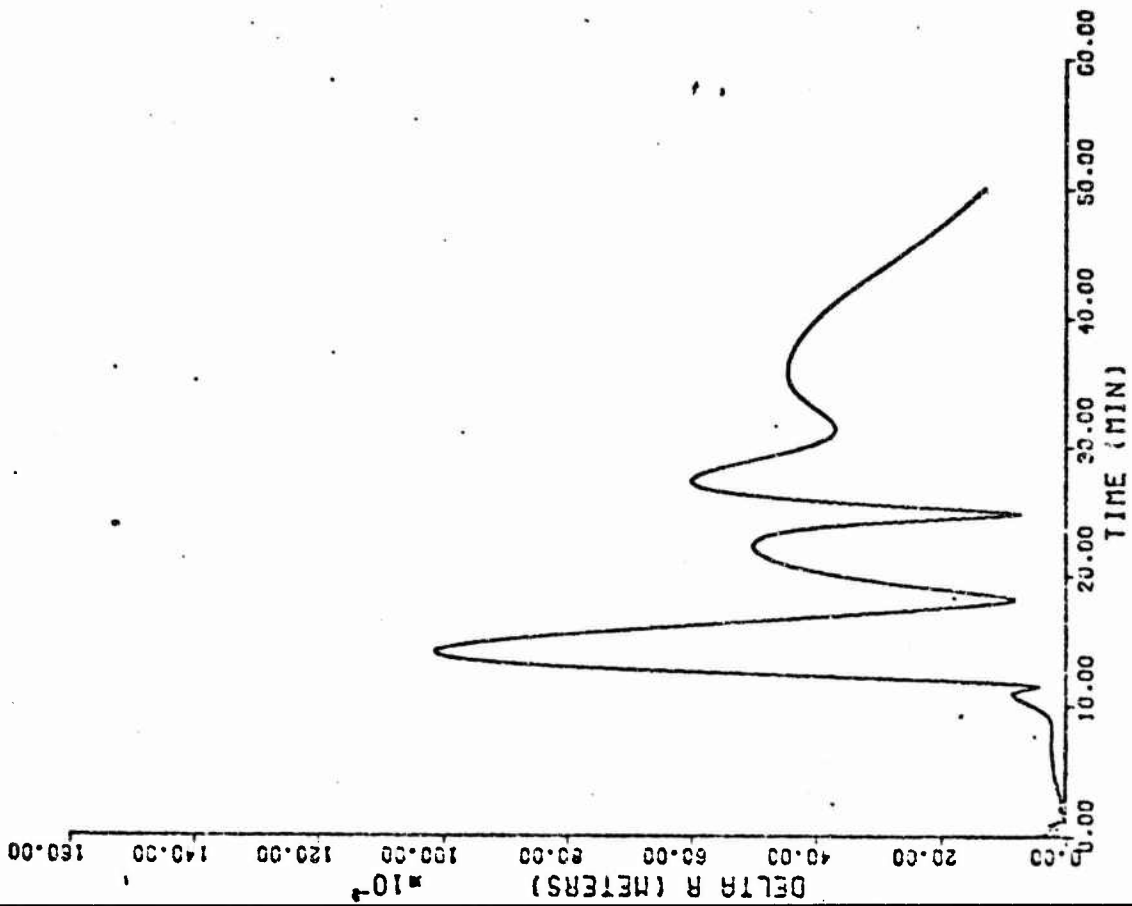


b. Velocity Error Norm

Figure 3. Error in Estimate with No Model Compensation ($I = 180^\circ$)



b. Velocity Error Norm

Figure 4. Error in Estimate with No
Model Compensation ($I = 150^\circ$)

a. Position Error Norm

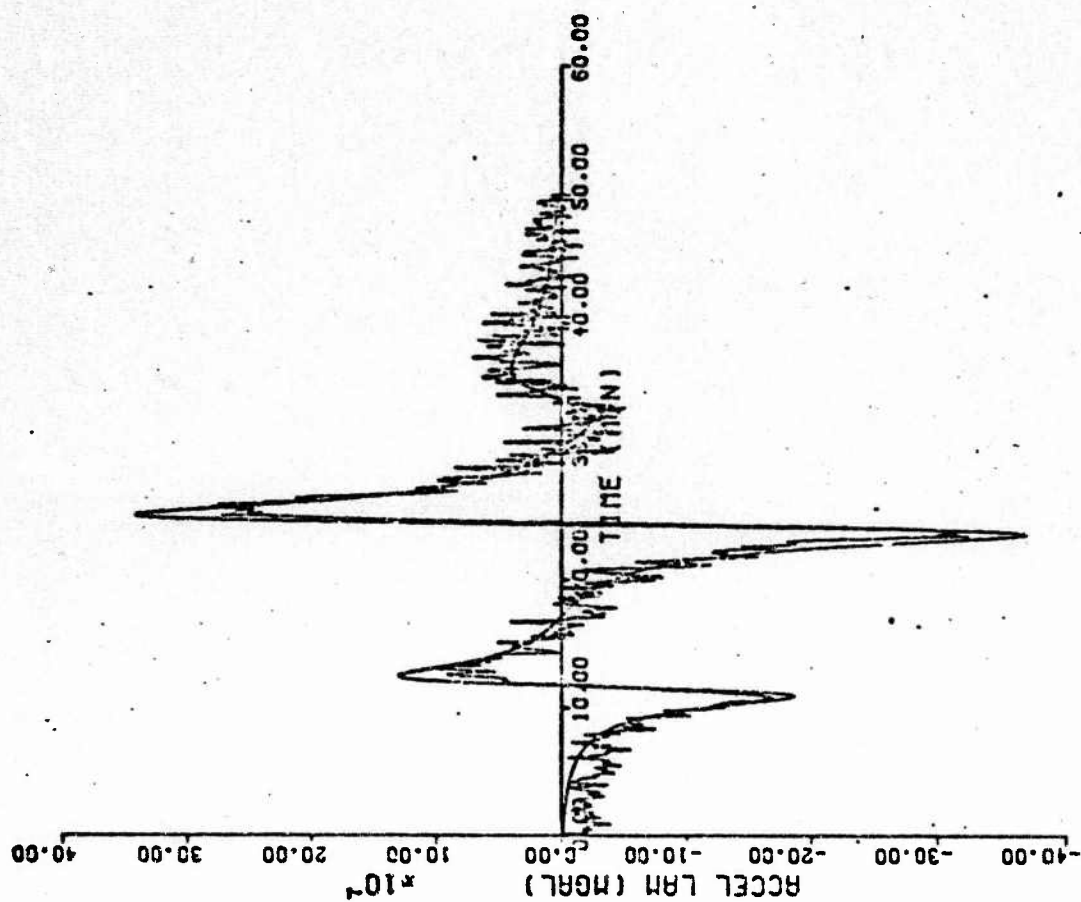
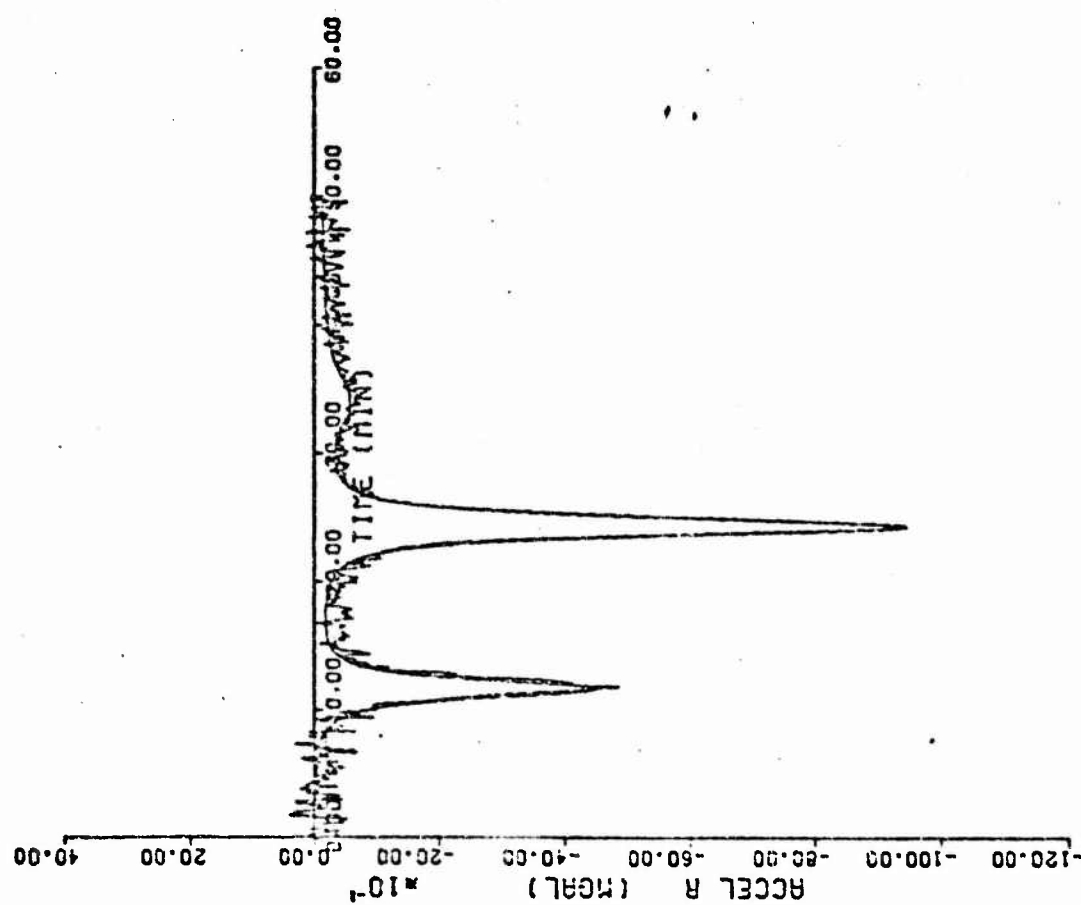
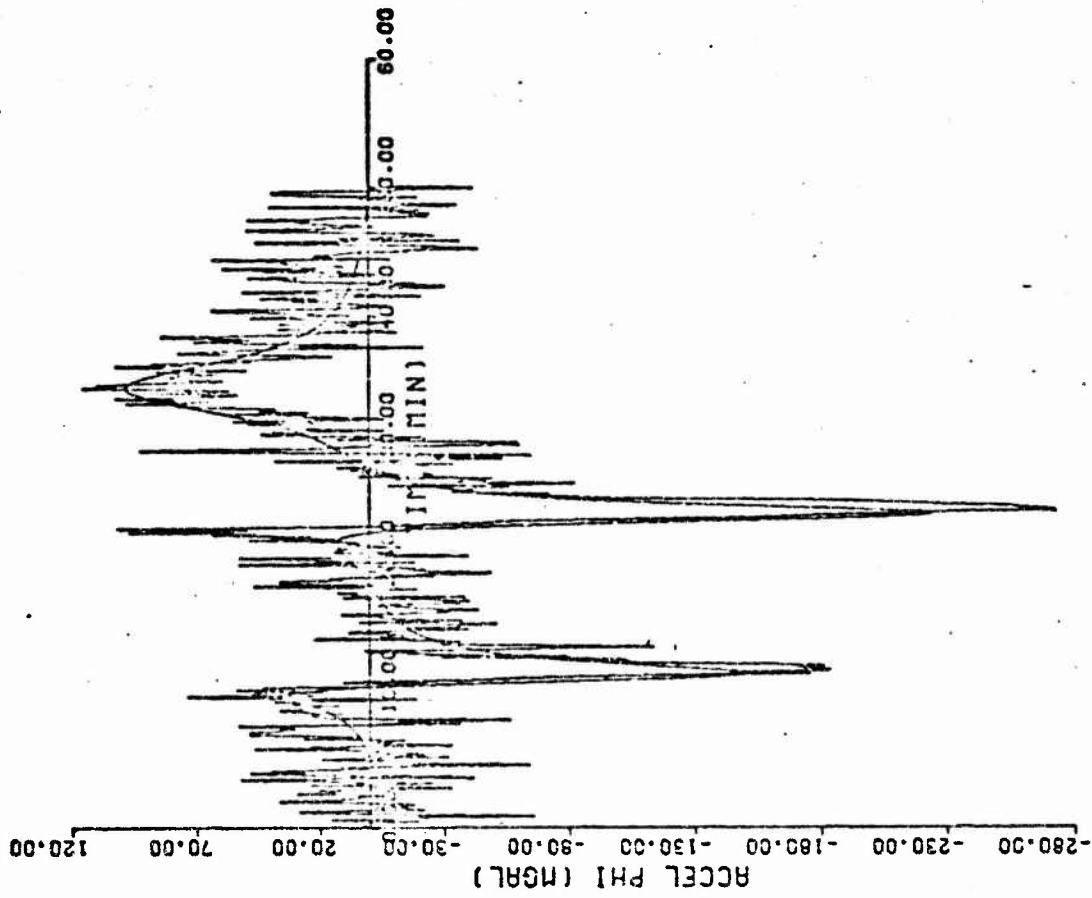
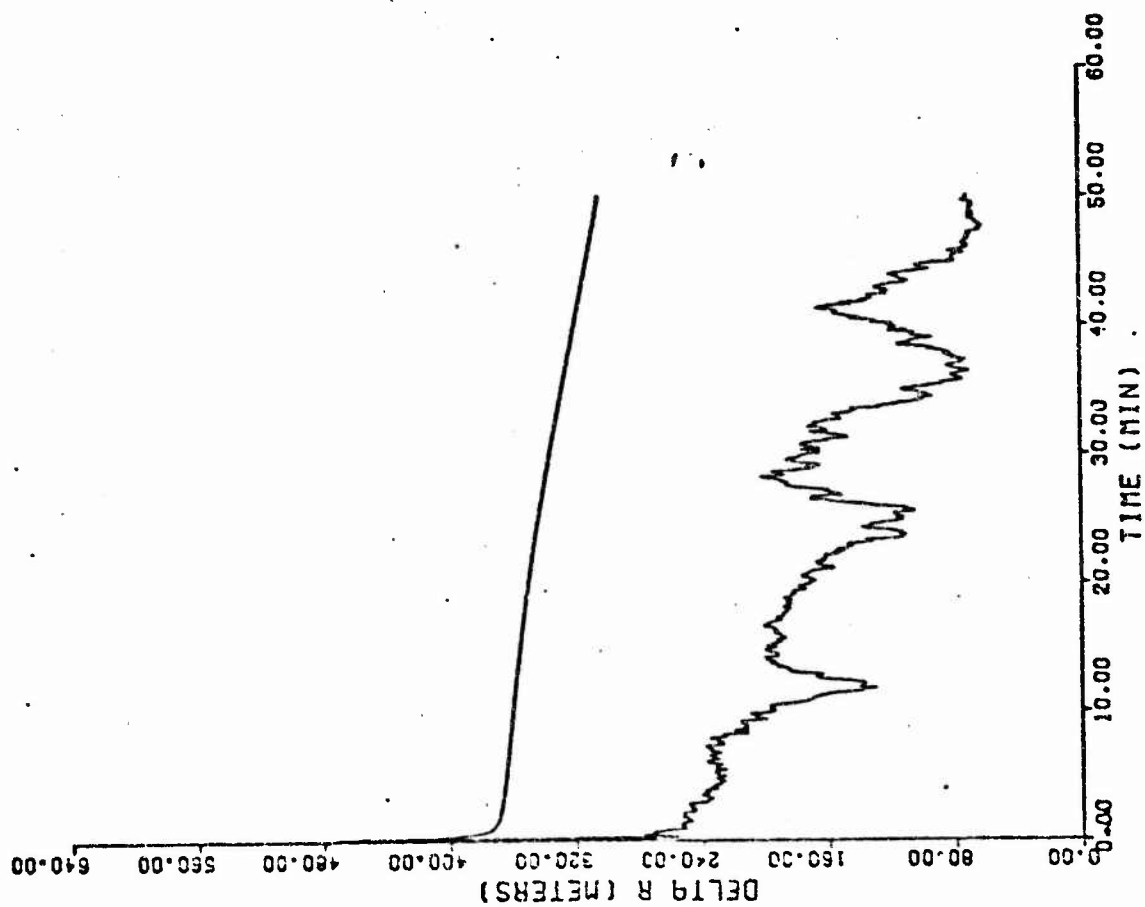
b. ϵ_λ Componenta. ϵ_r Component

Figure 5. $I' = 150^\circ$ Unmodeled Acceleration,
 $\sigma_p = 1.5$ mm/sec

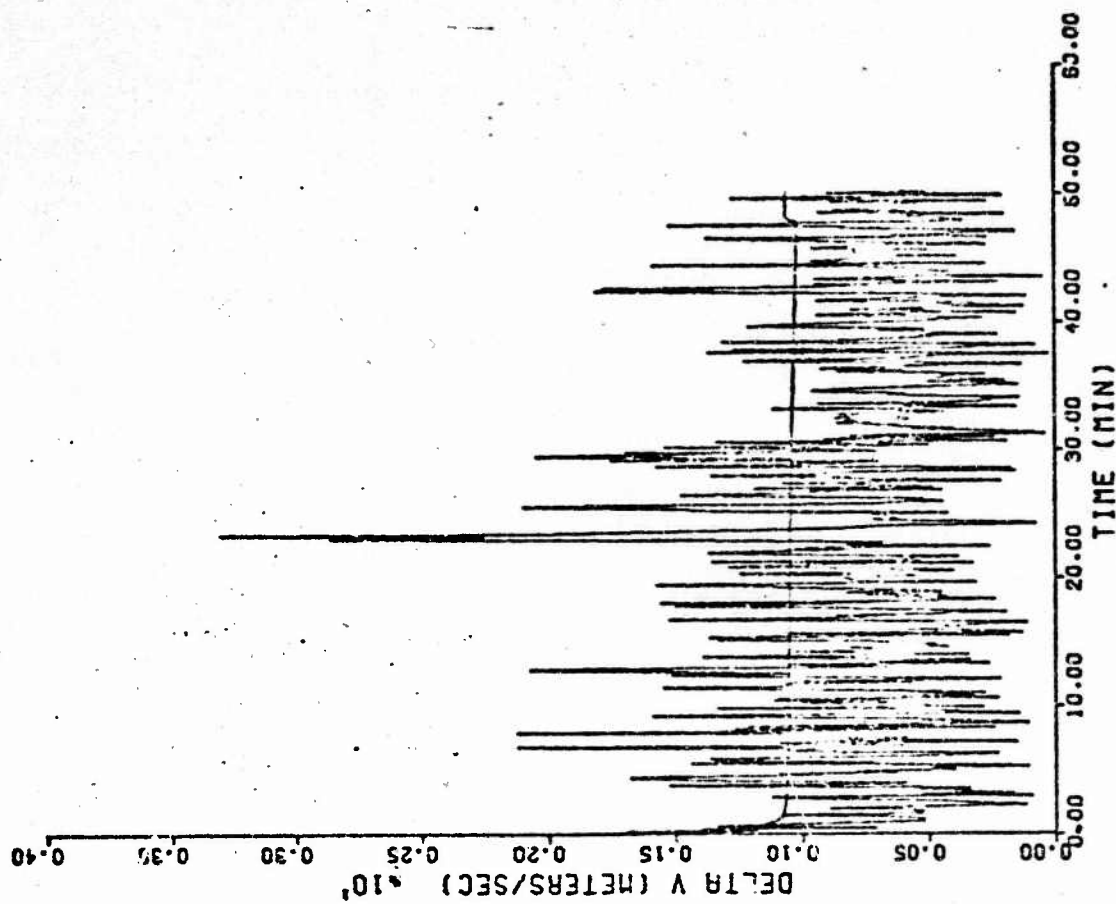


c. $\bar{\epsilon}_\phi$ Component

Figure 5. Continued

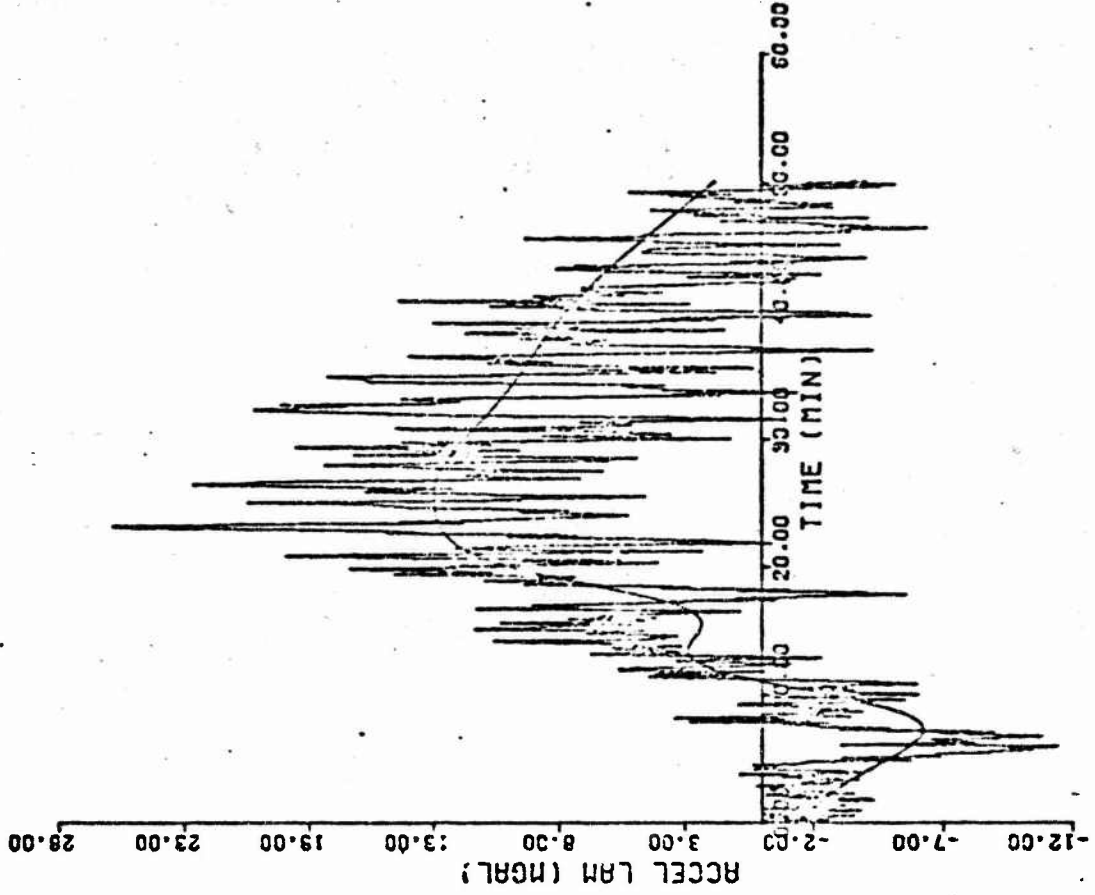


d. Position Error Norm

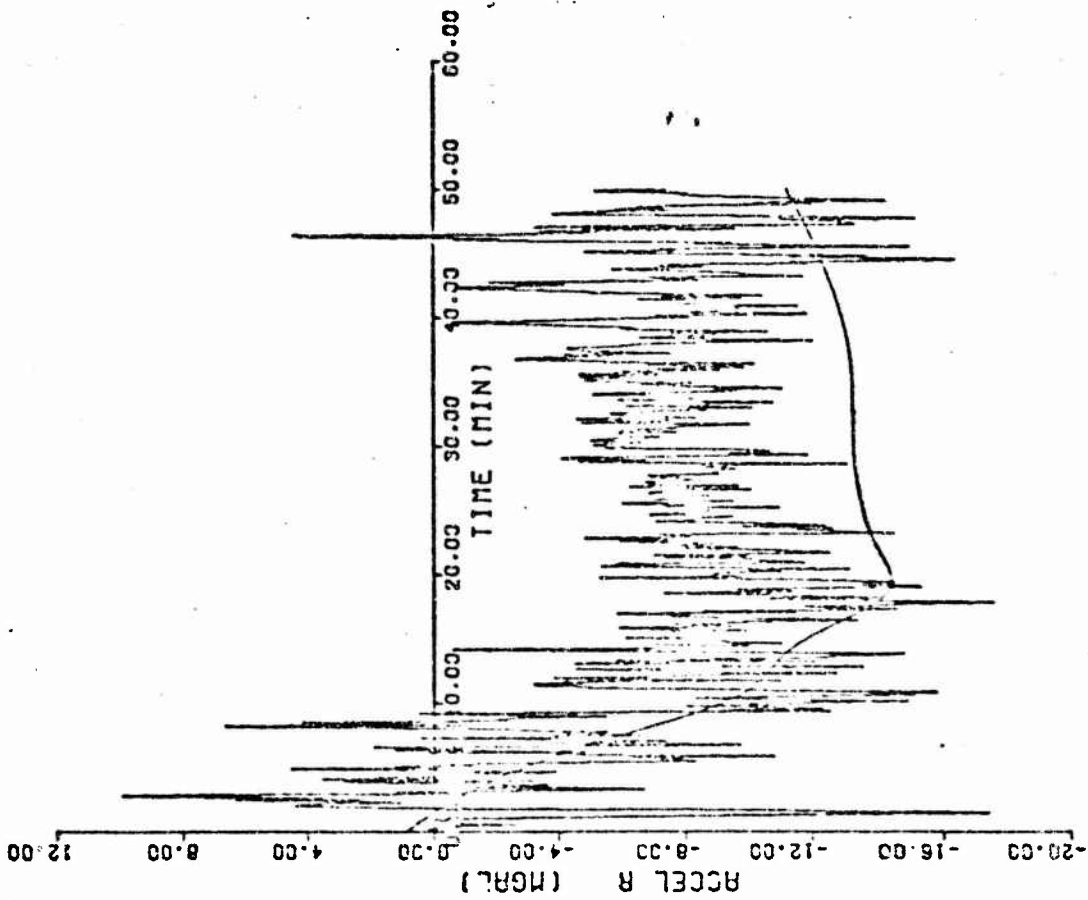


c. Velocity Error Norm

Figure 5. Continued

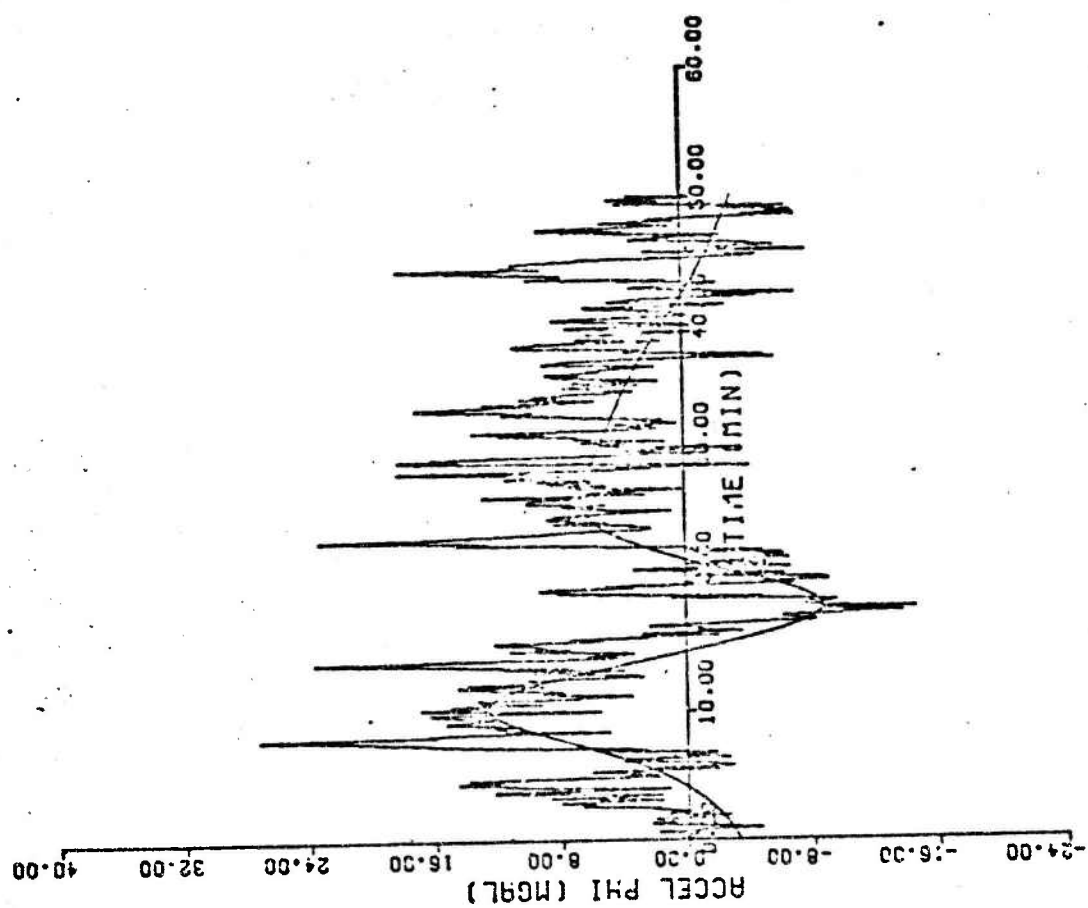


a. ϵ_x Component



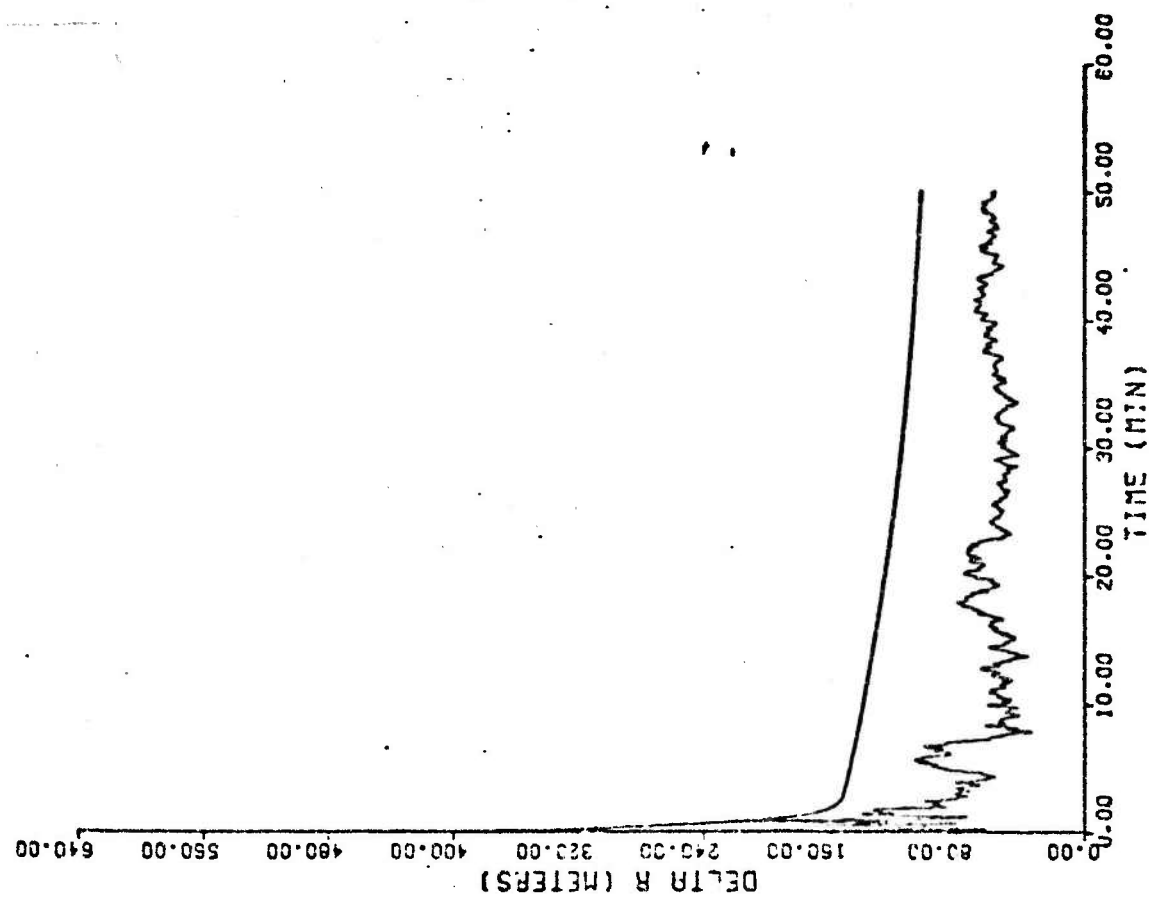
b. ϵ_y Component

Figure 6. $I = 0^\circ$ Unmodeled Acceleration,
 $\sigma_\theta = 1.5$ mm/sec

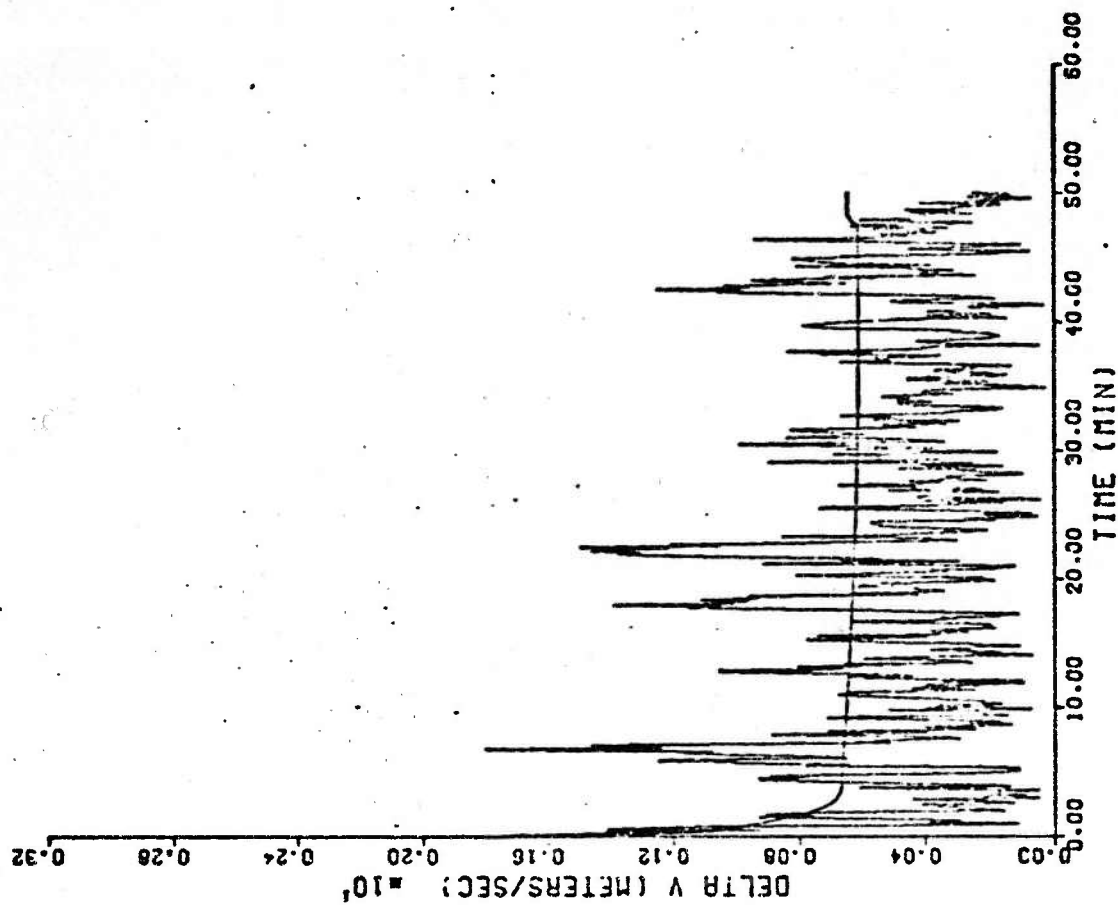


$\sigma. \bar{\epsilon}_\phi$ Component

Figure 6. Continued



d. Position Error Norm



e. Velocity Error Norm

Figure 6. Continued

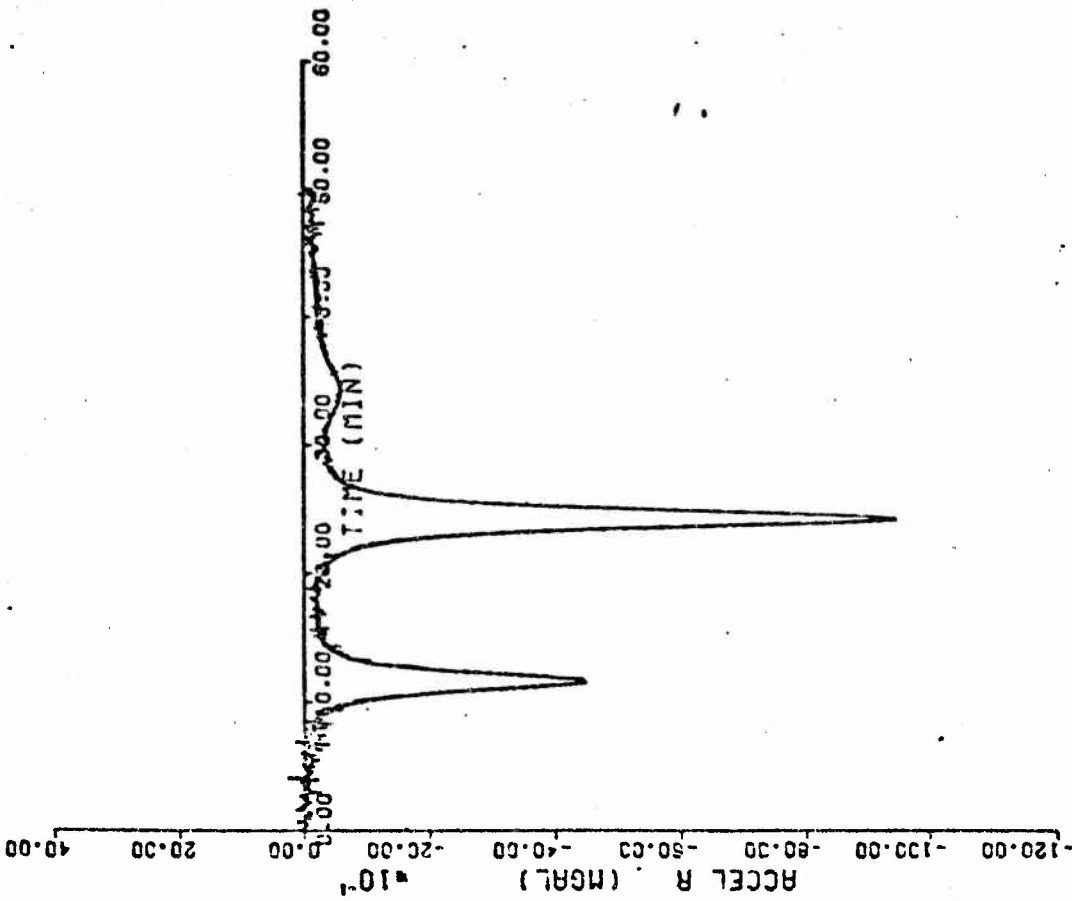
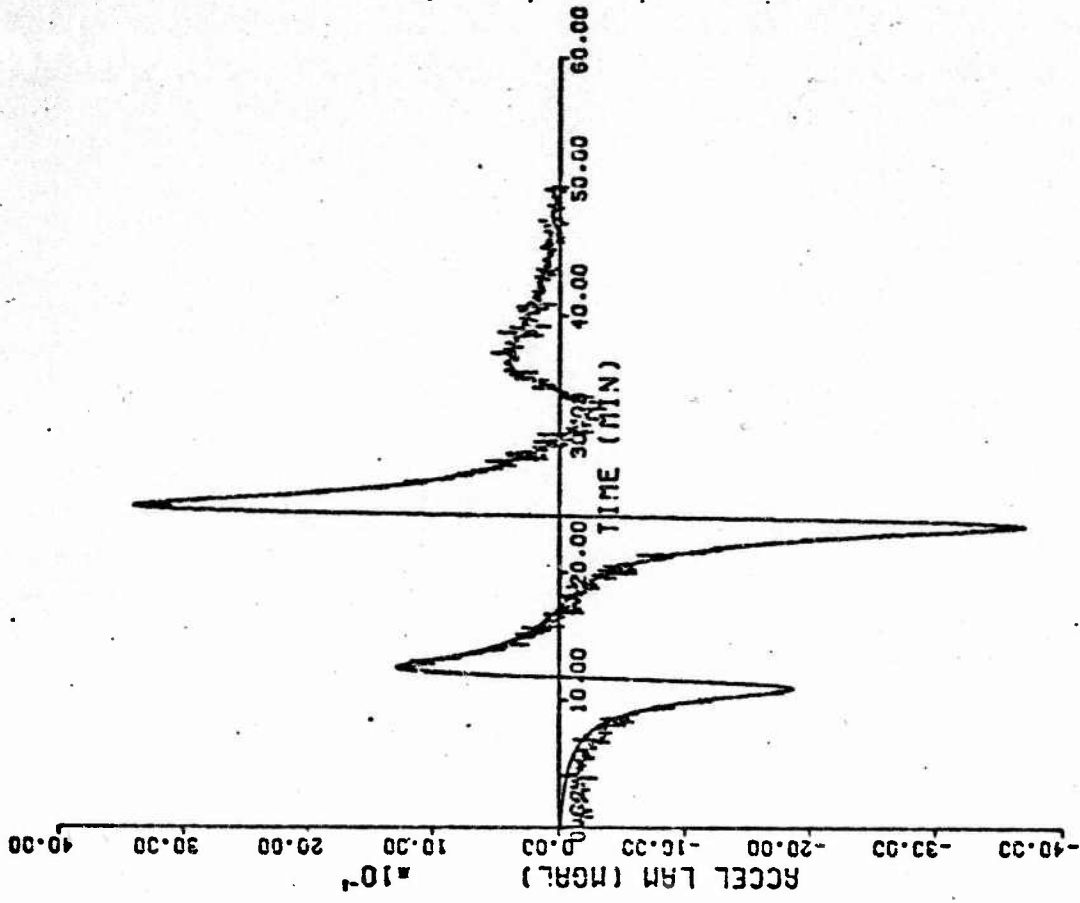
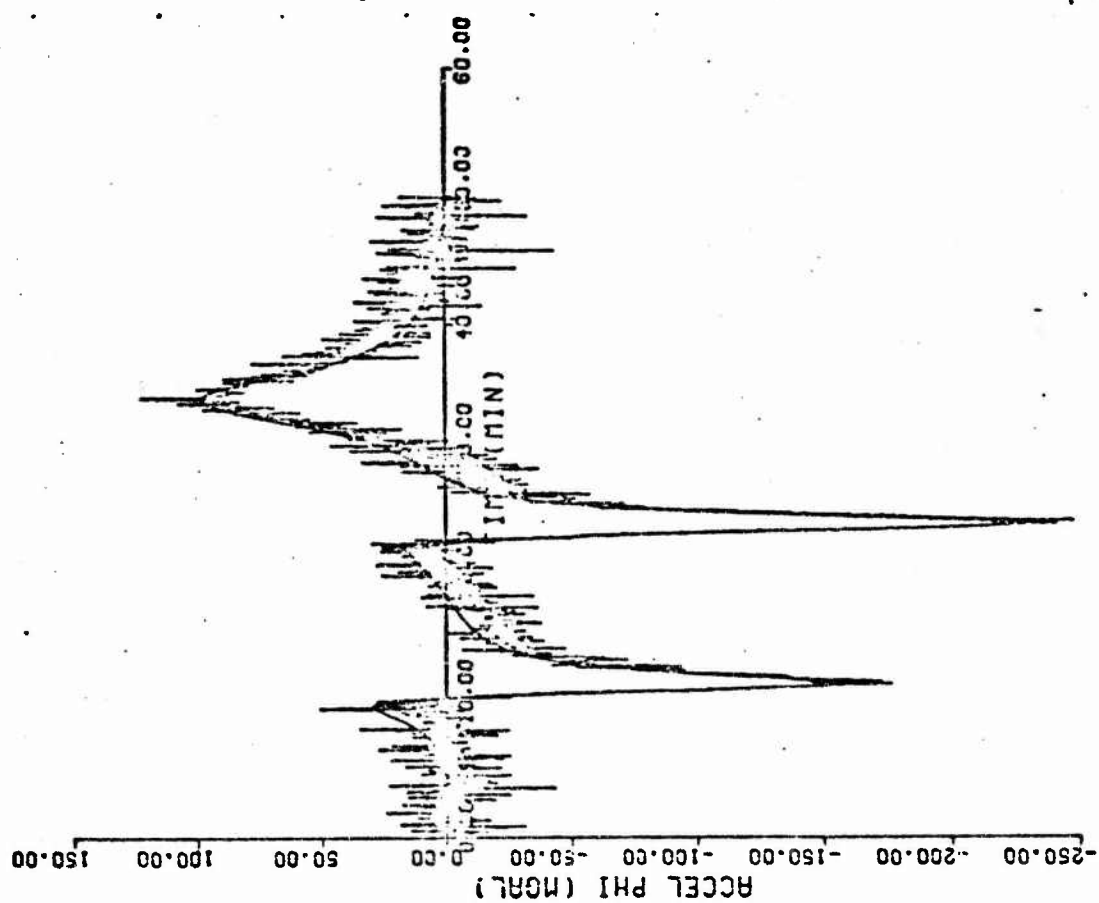
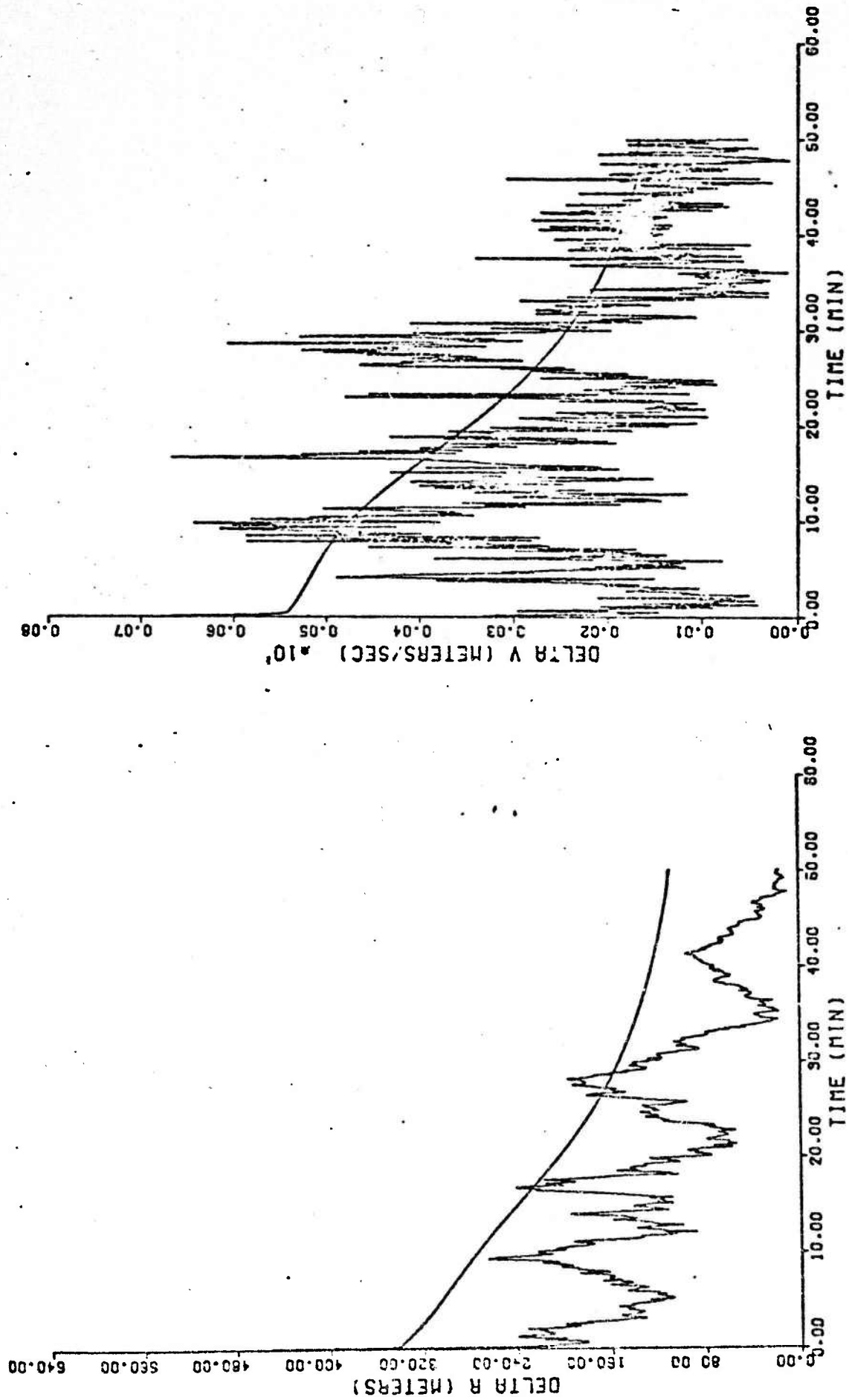
a. $\bar{\epsilon}_r$ Componentb. $\bar{\epsilon}_\lambda$ Component

Figure 7. $I = 150^\circ$ Unmodeled Acceleration
 $\sigma_\rho = 0.15 \text{ mm/sec}$



c. $\bar{\epsilon}_\phi$ Component

Figure 7. Continued



d. Position Error Norm

e. Velocity Error Norm

Figure 7. Continued